Asociación Argentina
de Mecánica Computacional

Mecánica Computacional Vol XLII, pp. 557-563
A. Caggiano, G. Etse, P. Folino, M. Goldschmit, M. Pucheta, M. Storti (Eds.)
P. Gamazo, P. Kler, S. Márquez Damián (Issue eds.)
Buenos Aires, November 11-14, 2025

PRELIMINARY NUMERICAL SIMULATION OF METHANE STEAM REFORMING IN POROUS CATALYTIC MEDIA

Toni Jadson da Silva[a], Jairo Aparecido Martins[a], Fabiano Fernandes Bargos[a] and Estaner Claro Romão[a]

[a]*Department of Basic and Environmental Sciences, Lorena School of Engineering, University of São Paulo, Research Group on Numerical Methods and Computational Engineering. Lorena, São Paulo, Brasil, ensinodecienciasexatas@usp.br, http://www.ensinodecienciasexatas.usp.br*

Keywords: Methane steam reforming; Hydrogen production; Porous media; Numerical simulation; Catalytic reactor.

Abstract. This work presents preliminary results of the numerical simulation of methane steam reforming in a porous catalytic medium, considering exclusively the global reaction with methane without the gas-shift reaction. The model was implemented in COMSOL Multiphysics based on the classical formulation of Darcy's law, the energy balance in porous media, and the transport of concentrated species. The analyses were performed in a simplified cylindrical geometry, varying the reactor length, the inlet temperature (800 and 900 K), and the CH_4/H_2O feed ratio. The results indicated that longer reactors and higher temperatures enhance methane conversion and hydrogen production, whereas the feed composition revealed trade-offs between relative conversion and absolute productivity. This study aligns with established trends in the literature and serves as the preliminary stage of an ongoing master's research project. Future work will involve extensive parametric analysis, integration of multiple reaction pathways, and a detailed investigation of process selectivity.

ISSN: 2591-3522 DOI: 10.70567/mc.v42.ocsid8624

1 INTRODUCTION

In recent years, growing concerns related to the energy crisis and climate change have driven the search for alternative and cleaner energy sources. In this context, hydrogen has emerged as a promising energy source due to its high energy density and renewable production potential, contributing to the reduction of greenhouse gas emissions and the mitigation of environmental impacts (Dincer and Acar, 2017; Furlan et al., 2019; Neves et. al., 2011).

Several methods for hydrogen production have been investigated; however, methane steam reforming stands out as one of the most consolidated routes. This process involves the reaction of methane with steam at high temperatures, leading primarily to the formation of hydrogen and carbon monoxide (Xu and Froment, 1989). The overall reaction can be expressed by Equation 1.

$$\mathbf{CH_4 + H_2O \rightarrow CO + 3H_2} \qquad (1)$$

The hydrogen obtained can be applied in several areas, including vehicular transportation through fuel cells, electricity generation, residential heating, and industrial chemical processes. It is therefore regarded as a clean fuel of great relevance for the energy transition (IEA, 2019).

Despite this potential, significant barriers to the widespread adoption of hydrogen remain, involving technical, economic, and infrastructure challenges (Zhao et al., 2021). Nevertheless, hydrogen is recognized as a strategic fuel for the future, owing to its versatility, high efficiency, and the fact that it does not release carbon dioxide during its utilization in fuel cells, thus becoming the focus of intense research and development efforts (Shabani and Aghakhani, 2020).

In this regard, the present study aimed to present the first results of methane steam reforming analysis over a nickel-based catalyst, as proposed by Zeppieri et al. (2010), considering exclusively the overall reaction presented in Equation 1. Other intermediate reactions were not considered in this preliminary stage.

2 MODEL EQUATIONS

For the case study presented here, which aims to analyze hydrogen production from methane steam reforming (Equation 1), the following governing equations are considered.

2.1 Darcy Law

Since a catalyst is employed, it is necessary to analyze the flow through porous media. Therefore, a classical formulation of Darcy's law is implemented, which relates the average flow velocity in the porous medium (known as Darcy velocity) to the pressure gradient, considering the medium permeability and the fluid viscosity. The expression is given as:

$$\mathbf{u} = -\frac{\kappa}{\mu}\nabla p \qquad (2)$$

where $\mathbf{u}$ is the superficial velocity (m/s); κ is the permeability of the porous medium (m²); μ is the dynamic viscosity of the fluid (Pa·s); and ∇p is the pressure gradient (Pa/m).

The gravitational term from the original Darcy's formulation was neglected since the reactor operates horizontally and the pressure gradients induced by buoyancy are orders of magnitude

smaller than those associated with the forced flow, thus having no significant effect on the velocity field.

Although Darcy's law was initially derived for incompressible liquid flow through porous media, it remains valid for gas flow under low Reynolds number and low Mach number conditions, where inertial and compressibility effects are negligible. In catalytic reactors, these conditions are typically satisfied due to the small pore sizes, moderate pressure gradients, and low flow velocities adopted in the model. Therefore, the classical Darcy formulation is appropriate for representing the gas phase behavior in this study.

Given that fixed and well-defined boundary conditions are adopted for this case study, as will be detailed throughout the text, the flow field presented here, as well as the temperature field (Section 2.2) and the concentration field (Section 2.3), are considered under steady-state conditions.

2.2 Heat Transfer in Porous Media

To analyze the temperature field within the porous medium (catalyst), the governing equation is expressed as follows:

$$\nabla \cdot \left(k_{eff} \nabla T\right) - \rho C_p \mathbf{u} \cdot \nabla T + Q = 0 \qquad (3)$$

where k_{eff} is the effective thermal conductivity of the medium (combining fluid and solid, in W/m·K); T is the temperature (K); ρ is the fluid density (kg/m³); C_p is the specific heat at constant pressure (J/(kg·K)); $\mathbf{u}$ is the Darcy velocity (m/s); and Q is the heat source or sink term (W/m³).

2.3 Transport of Concentrated Species in Porous Media

For the transport of concentrated species through the catalyst, the following governing equation is adopted:

$$\nabla \cdot \left(-D_{eff,i} \nabla c_i + \mathbf{u} c_i\right) + R_i = 0 \qquad (4)$$

where $D_{eff,i}$ is the effective diffusivity of species i (m²/s); $\mathbf{u}$ is the Darcy velocity (m/s); c_i is the concentration of species i; and R_i is the chemical reaction term of species i.

3 CASE STUDY

For the case study proposed in this work, hydrogen production will be analyzed considering only the overall chemical reaction presented in Equation 1, also proposed by Zeppieri et al. (2010), using a nickel-based catalyst (ICI Katalco 559 25-4MQ, supplied by Johnson Matthey).

Most of the parameters were directly taken from Zeppieri et al. (2010), while others were adapted or calculated, as follows:

- $\rho = 950$ kg/m^3 (Johnson Matthey, 2022);
- $\varepsilon = 0.45$ – porosity for the packed catalyst bed (calculated from the data of Zeppieri et al. (2010) and Johnson Matthey (2022));
- $C_p(T) = 607.164 + 0.126561 \cdot T$ [J/(kg·K)] (approximated function based on data obtained from JAEA (n.d.), for NiO in the range of 700–1000 K);

- $k_{eff} = 0.35$ W/(m·K) (Johnson Matthey, 2022);
- $\kappa = 8 \cdot 10^{-11}$ m^2 – permeability (calculated from a particle diameter reported by Zeppieri et al. (2010), $d_p = 200$ μm);
- $r = k \times C_{CH4}$ – reaction rate term in mol/(m^3·s) (Zeppieri et. al., 2010), where C_{CH4} is the CH_4 concentration;
- $k = Ae^{\left(-\frac{E_a}{RT}\right)}$ with $A = 7.26E + 07$ (s^{-1}), $E_a = 96.1$ kJ/mol and $R = 8.314462$ J/(kg·mol);
- μ, dynamic viscosity, is calculated by COMSOL through dl.mu variable. In this case variating between 2.65×10^{-5} and 3.28×10^{-5} $Pa \cdot s$;
- the mass diffusivity is calculated automatically by COMSOL via the Maxwell-Stefan model between species i and j;
- $Q = \varepsilon \cdot \text{chem. Qtot}$, where chem.Qtot represents the total heat of reaction generated or consumed per unit volume (total heat source term) due to chemical reactions.

All simulations presented in the following section, namely the numerical solution of Equations (1–4), were carried out using the COMSOL^{TM} Multiphysics platform.

4 RESULTS

For our case study, a "half-cylinder" geometry with length L and radius r_i was adopted. Symmetry was imposed at the central plane for all variables in Equations (2–4). In addition, the domain was assumed to be thermally insulated from the surroundings.

A half-cylindrical 3D geometry was adopted to exploit the plane of symmetry while still enabling a full three-dimensional velocity field, which is relevant for validating mesh convergence and assessing potential asymmetries in flow and temperature distributions near the inlet and outlet boundaries. Although an axisymmetric 2D model could reproduce the main physical trends with lower computational cost, the 3D representation ensures a more general formulation compatible with future extensions of the study, such as non-uniform boundary conditions or multi-channel reactor configurations.

For the flow field boundary conditions, $u_{inlet} = 0.02$ m/s was imposed at the inlet, and an zero-pressure was applied at the outlet. For the temperature field, an outflow condition $(-\mathbf{n} \cdot \mathbf{q} = \mathbf{0})$ was applied at the outlet, and two inlet temperature conditions were tested: 800 K and 900 K. For the concentration field, two mass fraction combinations were considered: the first with $CH_4 = 0.1$ and $H_2O = 0.9$, and the second with $CH_4 = H_2O = 0.5$, both with an outflow condition $\left(-\mathbf{n} \cdot \rho D_{eff,i} \nabla c_i = 0\right)$ at the outlet, that is, there is no diffusion back into the domain. At the reactor inlet, the mass fractions of the products CO and H_2 were set to zero, assuming that no conversion occurs upstream of the catalytic bed. This ensures that all product formation results exclusively from the reaction occurring within the porous catalyst domain. Finally, the radius was fixed at $r_i = 0.005$ m, while the reactor length L was varied between 0.01 and 0.025 m, with increments of 0.0025 m.

The results obtained allow for a systematic assessment of the influence of reactor geometry, inlet temperature, and the CH_4/H_2O feed ratio on the conversion of reactants and products.

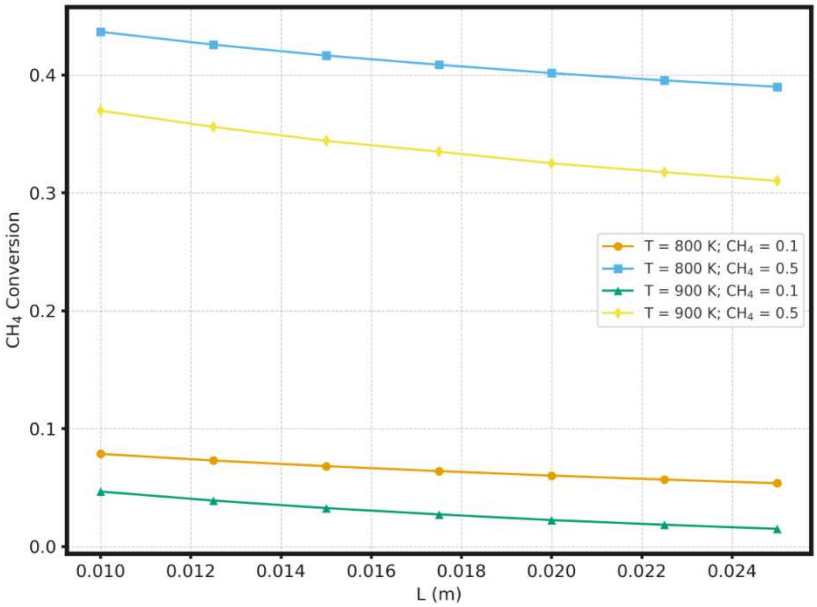

Figure 1: Effect of reactor length on CH_4 conversion for different inlet temperatures and feed compositions.

First, it is observed that increasing the reactor length *L* enhances CH_4 conversion (Figure 1). The longer residence time favors the occurrence of the reforming reaction, also leading to higher production of H_2 (Figure 2) and CO (Figure 3). This behavior confirms that longer reactors exhibit greater reaction efficiency, although the increased formation of CO may require additional purification steps in practical applications.

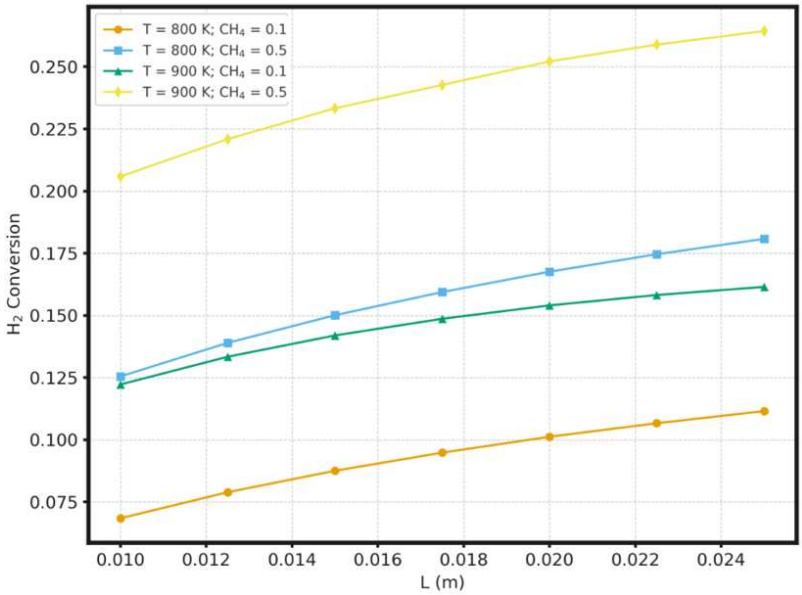

Figure 2: Effect of reactor length on H_2 production for different inlet temperatures and feed compositions.

Regarding the inlet temperature, the condition of 900 K proved to be more favorable than 800 K, leading to higher methane conversions. This result is consistent with the endothermic nature of steam reforming, in which an increase in temperature shifts the equilibrium toward higher conversions. Consequently, hydrogen production increases and CO formation is intensified, highlighting temperature as a critical parameter for process control.

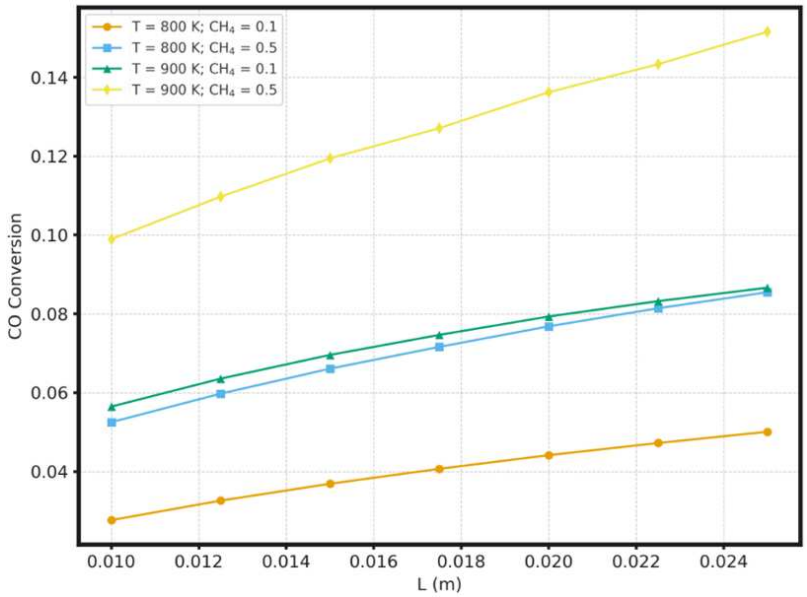

Figure 3: Effect of reactor length on CO production for different inlet temperatures and feed compositions.

As for the feed ratio, the methane-diluted mixture ($CH_4 = 0.1$; $H_2O = 0.9$) exhibited higher relative CH_4 conversion, since the smaller initial amount of methane results in a significant fraction being consumed along the reactor. In contrast, the equimolar condition ($CH_4 = H_2O = 0.5$) resulted in a lower conversion percentage but produced higher absolute amounts of H_2 and CO, owing to the greater initial availability of methane. This outcome highlights the trade-off between conversion efficiency and overall productivity, a central aspect in the design of reactors at the industrial scale.

In general, it is observed that reactor length directly influences the conversion rate, higher temperature enhances the overall efficiency of the process, and the CH_4/H_2O feed ratio plays a decisive role in selectivity. These trends are consistent with previous studies on steam reforming and demonstrate the consistency of the proposed modeling approach, even though it is simplified by the exclusion of parallel reactions such as the water–gas shift.

5 CONCLUSIONS

The present work presented preliminary results of the numerical simulation of methane steam reforming in a porous catalytic medium, considering exclusively the global hydrogen production reaction (Equation 1). The results showed that increasing the reactor length promotes higher CH_4 conversion, accompanied by greater H_2 and CO formation. It was also verified that raising the inlet temperature from 800 K to 900 K intensifies the conversions, consistent with the endothermic nature of the reaction. In addition, the CH_4/H_2O feed ratio demonstrated a significant influence: the methane-diluted condition (0.1/0.9) achieved higher relative conversion, whereas the equimolar mixture (0.5/0.5) resulted in greater absolute product yields, highlighting the trade-off between efficiency and productivity.

These results corroborate trends reported in the literature and validate the consistency of the adopted numerical model, even though it was simplified by excluding parallel reactions such as the water–gas shift. However, as this is a preliminary study linked to an ongoing master's thesis, further developments are still required. Among them are the expansion of the range of analyzed parameters (temperature, inlet velocity, and geometric dimensions), the inclusion of multiple chemical reactions, a more detailed assessment of catalyst properties, and the analysis of hydrogen selectivity in relation to by-product formation.

Thus, this work constitutes an initial step toward understanding the modeled process, providing a foundation for subsequent project stages and for consolidating an optimization methodology aimed at sustainable hydrogen production.

REFERENCES

Dincer I., and Acar C., Review and evaluation of hydrogen production methods for better sustainability. *International Journal of Hydrogen Energy*, 42:3471–3482, 2017. http://doi.org/10.1016/j.ijhydene.2016.06.043

Furlan J., Martins J. A., Romão E. C., Dispersion of toxic gases (CO and CO2) by 2D numerical simulation, Ain Shams Engineering Journal, Volume 10, Issue 1, 2019, Pages 151-159. https://doi.org/10.1016/j.asej.2018.03.010.

IEA – International Energy Agency, *The Future of Hydrogen: Seizing today's opportunities*. Paris: IEA, 2019. https://www.iea.org/reports/the-future-of-hydrogen

JAEA (Japan Atomic Energy Agency), *Thermodynamic data – NiO*. 2025. Access in 09/03/2025. https://thermodb.jaea.go.jp/data/en/td/NiO.html

Johnson Matthey, *Steam reforming catalysts*. 2022. Access in 09/03/2025. https://matthey.com/documents/161599/348563/JM+Steam+reforming+catalysts+Product+Brochure.pdf/99deb020-f1af-f436-c6b3-a3557ad2499e?t=1664979352415

Neves, O. A., Romão, E. C., Campos-Silva, J. B. and Moura, L. F. M. (2011), Numeric simulation of pollutant dispersion by a control-volume based on finite element method. Int. J. Numer. Meth. Fluids, 66: 1073-1092. https://doi.org/10.1002/fld.2296

Shabani B., and Aghakhani A., Hydrogen as a fuel for transportation: Technology, infrastructure and perspectives. *Renewable and Sustainable Energy Reviews*, 134:110196, 2020. http://doi.org/10.1016/j.rser.2020.110196

Xu J., and Froment G.F., Mathematical modeling of monolithic catalysts for steam reforming of methane. *AIChE Journal*, 35:88–96, 1989. http://doi.org/10.1002/aic.690350109

Zeppieri M., Villa P.L., Verdone N., Scarsella M., and De Filippis P., Kinetic of methane steam reforming reaction over nickel- and rhodium-based catalysts. *Applied Catalysis A: General*, 387:147–154, 2010. http://doi.org/10.1016/j.apcata.2010.08.017

Zhao J., et al., Recent advances in hydrogen production: catalysis and process development. *Chemical Engineering Journal*, 421:129804, 2021. http://doi.org/10.1016/j.cej.2020.129804